Volume 10 Number 4
2017
doi: 10.7289/V52805PH

Quarterly

Newsletter–Winter 2017 Issue

GSICS Global Space-based Inter-Calibration System

Manik Bali, Editor

CMA • CNES • EUMETSAT • IMD • ISRO • JAXA • JMA • KMA • NASA • NIST • NOAA • ROSHYDROMET • USGS • WMO

In This Issue

Articles

News in This Quarter

Announcements

Figure. 1*. GOES-16 Full disk image
For detailed description click here.

Credits: geospatialworld.net

Initial Data from GOES-16 ABI

by Xiangqian Wu (NOAA)

The GOES-16 Post-Launch Test (PLT) started formally on December 8, 2016, when outgassing was in progress. On January 6, 2017, the ABI opened its door and saw first light. Followed the detector cool down and other preparations, a set of images were obtained on January 15, 2017 for initial public release on January 23, 2017. Figure 1 is a full disk image composited from measurements by several ABI bands to simulate the color as one would see near the surface ("true color").

On February 28, 2017, GOES-16 ABI Level 1b product achieved Beta maturity successfully, and the Post-Launch Product Tests (PLPT) started formally. Only limited information has been authorized for release before PLPT concludes with Provisional maturity, which is scheduled for June. Table 1 shows the signal-to-noise ratio (SNR, average of all detectors for the band) for the six ABI visible and near infrared (VNIR) bands at the beginning of life (BOL), as determined during on-board solar calibration using partial-aperture observations of solar diffuser illuminated by the Sun.

Figure 2 shows the net equivalent delta-temperature (NEdT, average of all detectors for the band) for the ten Infrared IR) bands at BOL.

The NEdT was computed from radiance noise for a target temperature of 300 K in most cases. The radiance noise was determined during on-board IR calibration using the onboard blackboard or Infrared Calibration Target (ICT).

In addition to the substantially improved performance for noise, ABI calibration is also stable. Figure 3 shows the counts (left panel) and gain (right panel) of five solar calibrations for the six visible and near infrared bands of ABI. The first three occurred within 15 minutes; the next two are each two days apart, with similar

Doi: 10.7289/V52805PH
GSICS Quarterly: Winter Issue 2017 Volume 10, No. 4, 2017

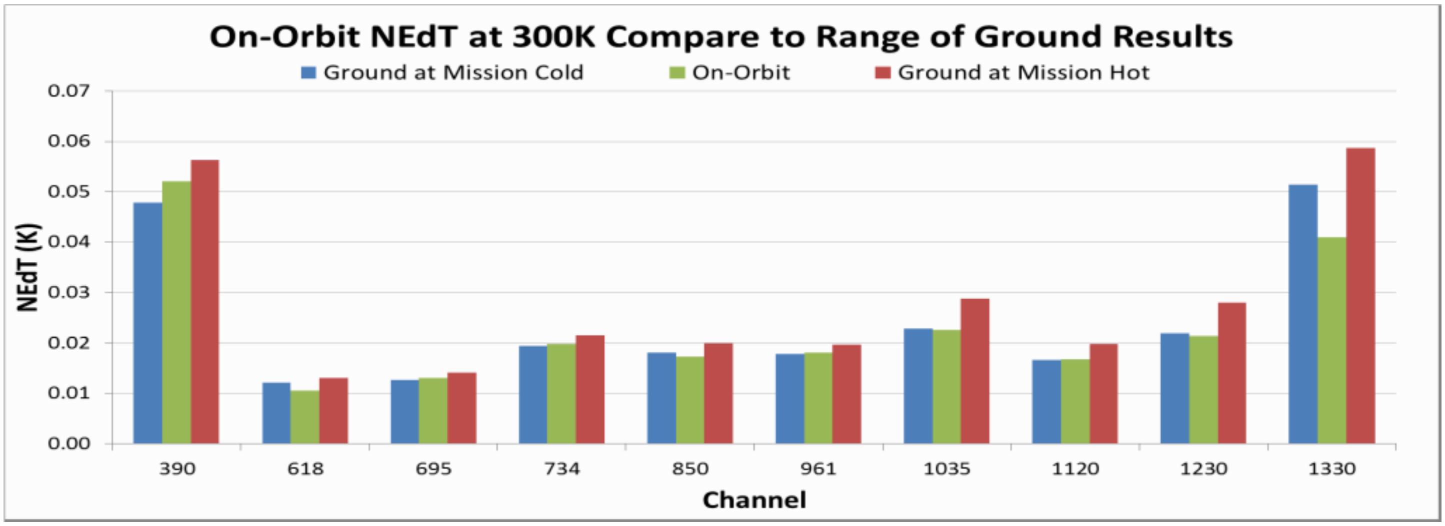

Figure 2: ABI BOL NEdT for its IR bands. Courtesy of Griffith et al 2017

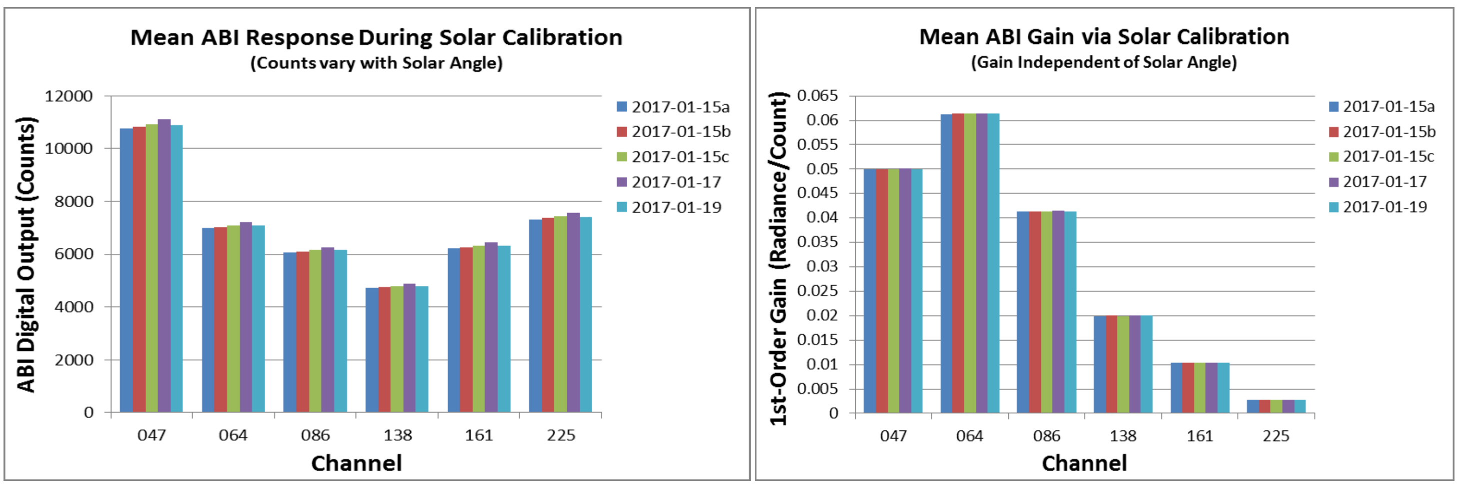

Figure 3: ABI solar calibration stability. Courtesy of Griffith et al 2017.

Wavelength	On-Orbit SNR†
0.47	1196
0.64	508
0.86	784
1.38	1124
1.61	640
2.25	1137

Table 1: ABI BOL SNR for its VNIR bands. Courtesy of Griffith et al 2017.

elevation angle of the Sun. The count values varied, primarily due to changes in the angles of incidence (AOI) at the times of observations, but the on ground Characterization of the ABI instrument was able to account for those effects such that the instrument gain has been stable (right panel). Following the Beta maturity of GOES-16 ABI Level 1b and Cloud and Moisture Imagery (CMI) products, these data have been routinely distributed to internal users since March 1, 2017. The GOES-R Calibration Working Group will work with users, in addition to Flight and Ground vendors and operators, to improve ABI data quality and utilities.

References:

Griffith, P., W. J. Lebair, T. J. Schmit, X. Wu, and J. Van Naarden, 2017: Initial on-orbit Advanced Baseline Imager (ABI) performance observations. *American Meteorological Society, Seattle, WA, January 25, 2017*

Figure 1*: *Full-disk image of the Western Hemisphere captured from NOAA GOES-16 satellite at 1:07 pm EST on Jan. 15, 2017 and created using several of the 16 spectral channels available on the satellite's sophisticated Advanced Baseline Imager. The image, taken from 22,300 miles above the surface, shows North and South America and the surrounding oceans. Credits: NOAA*

Discuss the Article

Doi: 10.7289/V52805PH
GSICS Quarterly: Winter Issue 2017
Volume 10, No. 4, 2017

Improvements to the Suomi NPP Ozone Mapper Profiler Suite's Sensor Data Records

by Chunhui Pan, Fuzhong Weng, Trevor Beck, Lawrence Flynn and Shouguo Ding, NOAA

Abstract: The Ozone Mapping and Profiler Suite (OMPS), one of the five instruments onboard the Suomi National Polar-orbiting Partnership (S-NPP) satellite, has been successfully operating for over five years [1, 2, and 3]. Recently, a major change in the on-orbit spectral wavelength calibration has been applied to the sensor characterization to improve the sensor spectral registration for each spatial Instantaneous Field of View (IFOV). This improvement allows the OMPS Sensor Data Records (SDRs) to reach the 2% wavelength-dependent albedo error performance requirement, for most of the channels across all of the IFOVs.

Keywords: Suomi-NPP, OMPS, radiometric calibration, remote sensing, wavelength.

Introduction

The OMPS nadir-viewing system has two hyperspectral Ultraviolet (UV) imaging spectrometers, the Nadir Mapper (NM) operating from 300 to 380 nm for nadir total column ozone observations and the Nadir Profiler (NP) operating from 250 to 310 nm for nadir profile ozone observations. Both spectrometers were designed to measure the UV radiance backscattered by the Earth's atmosphere and surface as well as the extraterrestrial solar irradiance. The ratios of the measured Earth radiances to the observed solar irradiances, normalized radiances (NR), are the principle SDR product used to generate the OMPS Environmental Data Records (EDRs) [4].

1. Wavelength calibration

The OMPS wavelength calibration defines the spectral scale of each OMPS spectrometer as a function of spatial position for each CCD pixel located on the focal plane. The first on-orbit wavelength calibration was conducted in 2013 when it was found that the sensor dichroic filter had experienced a spectral shift during the sensor transition from ground to orbit. Further study has revealed that the NM spectral wavelength scale shifts from 0.02 nm to 0.06 nm during each orbit. The amount of the shift for each spectral pixel in a spatial row has little wavelength dependence but the shift amounts vary with the cross-track IFOVs. The shift's orbital dependence tracks the instrument temperature gradients and increases towards the edge of the CCD for spatial cross-track positions as shown in figure 1. Without correction, these wavelength shifts create approximately 1% errors in radiance leading to 2% uncertainty in the retrieved ozone profiles' error budget. Corrections of the wavelength scales for the ground-to-orbit shifts were made by comparison of the sensor observed solar spectrum with the synthetic solar spectrum [3]. The

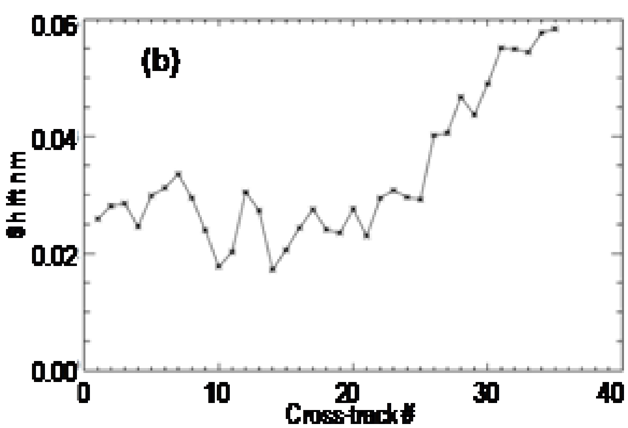

Figure 1. EV spectral average shifts for the mean dayside signal relative to the solar top-of-orbit (Northern terminator) wavelength scales versus cross-track position.

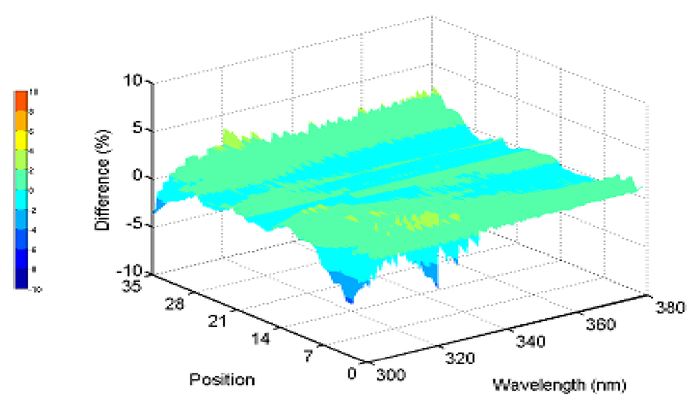

Figure 2. Normalized radiance error is computed between OMPS and the EOS-AURA MLS using the TOMRAD radiative transfer model. Errors are < 2% for most channels, except for individual channels at the far end of the CCD. Soft calibrations are implemented to eliminate this residual error at the EDR level.

Return to Page 1

Doi: 10.7289/V52805PH
GSICS Quarterly: Winter Issue 2017 Volume 10, No. 4, 2017

along-orbit Earth radiance wavelength scale corrections and calibration are evaluated through comparisons of the normalized radiances between OMPS and Radiative Transfer (RT) forward model results using ozone profiles from the Microwave Limb Sounder (MLS) sensor flying on EOS Aura [4]. The MLS data are used to establish a standard for the OMPS sensor through RT forward modeling as follows. Data collected from OMPS and MLS measurements were co-located within 50 km at OMPS viewing conditions between -20° and +20° north latitude and the TOMRAD forward model was used to generate full spectral measurement estimates by using the ozone profiles, instrument viewing geometry and the 331 nm effective reflectivity. Figure 2 shows relative difference between the MLS predictions and the OMPS NM radiance/irradiance ratios versus wavelength and cross-track spatial IFOVs. It is noted that a significant improvement has been made through the calibration adjustments; the albedo error is reduced from 5% (not shown) to less than 2% for the most of NM channels at each IFOV, except for few individual channels at the far off-nadir IFOVs where error residuals are slightly above 2%.

Summary

The sensor in-flight performance has been greatly improved through sensor on-orbit wavelength calibration. The NM sensor is performing within its calibration requirements and is generating high quality SDRs for use in meteorological and climate/global change research. The calibration lessons learned from the OMPS present reasonable and feasible opportunities for improving the future JPSS OMPS orbital calibration.

Acknowledgments

We would like acknowledge NASA OMPS PEATE team for sharing calibration data and analysis, and calibration tools for our study. This work was also supported by the NOAA JPSS program.

References

[1] Pan C., L. Flynn, X. Wu, R. Buss, (2014): Suomi National Polar-orbiting Partnership Ozone Mapping Profiler Suite Nadir instruments in-flight performance, *J. Appl. Remote Sens*. 8, 1, 083499. DOI: 10.1117/1.JRS.8.083499.

[2] Pan, C., M. Kowalewski and R. Buss, L. Flynn, X. Wu M. Capani and F. Weng, (2013), Performance and Calibration of the Nadir Suomi-NPP Ozone Mapping Profiler Suite from Early-Orbit Images", *IEEE Journal of Selected Topics in Applied Earth Observations and Remote Sensing*, DOI:10.1109/JSTARS.2013.2259144.

[3] Pan, C., L. Flynn, (2015), Solar observation of Ozone Mapping and Profiler Suite nadir system during the first 3 years of on-orbit operation. *J. Appl. Remote Sens*. 9,1, 094095, doi:10.1117/1.JRS.9.094095.

[4] C. J. Seftor, G. Jaross, M. Kowitt, M. Haken, J. Li, and L. E. Flynn, "Post launch performance of the Suomi National Polar-orbiting Partnership Ozone Mapping and Profiler Suite (OMPS) nadir sensors", DOI: 10.1002/2013JD020472.

Discuss the Article

Inter-calibration of VIRR/FY-3A/B split-window channels with AIRS/Aqua and IASI/Metop-A measurements

by Geng-Ming Jiang, Zhong-Yi Wang (Fudan University), and Junbang Wang (Chinese Academy of Sciences)

The Visible and InfraRed Radiometers (VIRRs) on board the new generation of Chinese meteorology satellites FengYun (FY) 3A/B/C have been operational for several years, since they were sequentially launched into space in May 2008, November 2010, and September 2013, respectively. Each VIRR has ten channels ranging from the visible to infrared spectrum with a nominal spatial resolution of 1.1 km at nadir. The channels 4 (centered at 10.8 μm) and 5 (centered at 12.0 μm) are two split-window bands. VIRR is the only instrument on FY-3 that can provide high spatial resolution and narrow band infrared window measurements. These can be used for cloud or fog detection and estimation of cloud properties, surface temperature and Earth radiation budget. After operation for several years in space, it is necessary to assess the performance of the VIRR's on-orbit radiometric calibration, and to try to correct it for continued use in applications.

An inter-calibration method for instruments on polar-orbit satellites was proposed by Jiang (2010), and is now improved and has been used to inter-calibrate the two split-window channels of VIRR/FY-3A/B in June and December of years from 2010 to 2013 (Jiang et al., 2016). The Atmospheric InfraRed Sounder (AIRS) on Aqua and Infrared Atmospheric Sounding Interferometer (IASI) on Metop-A were used as reference instruments, because of their fine spectral channels and excellent calibration accuracy.

Under the collocated, coincident and co-angled viewing conditions, the expected accurate measurements in VIRR/FY-3A/B channels 4 and 5 can be predicted as a function of the hyperspectral radiances through convolution with each channel's Spectral Response Function (SRF), i.e.,

$$L_{i,c} = \int_{v_1}^{v_2} L(v) f_i(v) \mathrm{d}v \Big/ \int_{v_1}^{v_2} f_i(v) \mathrm{d}v \quad ...(1)$$

where $L_{i,c}$ is the convolved hyperspectral radiance in a VIRR/FY-3 channel i (i=4 or 5), $L(v)$ is the hyperspectral radiance at frequency v, $f_i(v)$ is the SRF of VIRR/FY-3 channel i, and v_1 and v_2 are the lower and upper frequency limits of the SRF, respectively.

The relationship between the collocated, coincident and co-angled convolved hyperspectral radiances and the radiances in the broad channel can be well modelled by a linear function

$$L_{i,c} = a_i L_i + b_i \quad ...(2)$$

in which L_i is the radiance in VIRR/FY-3 broad channel i, and a_i and b_i are two unknown inter-calibration coefficients, determined through linear regression on a sufficient number of matching measurements.

With full consideration of satellites' orbits and viewing geometry, an Arctic region (180°W—180°E, 60°N—90°N) was selected as the intercalibration area. An x-y Cartesian coordinate grid was setup as follows: the origin is located at North Pole (90°N), and x and y axes point to (90°W, 60°N) and (0, 60°N), respectively. The transformation from longitude (α) and latitude (β) in degree to x and y is given by

$$\begin{cases} x = (90^{\circ} - \beta)\cos\zeta \\ y = (90^{\circ} - \beta)\sin\zeta \end{cases} \quad ..(3)$$

with

$$\zeta = \begin{cases} \vartheta + 90^{\circ}, & \text{if } \vartheta \le 270^{\circ} \\ \vartheta - 270^{\circ}, & \text{if } \vartheta > 270^{\circ} \end{cases}$$ and

$$\vartheta = \begin{cases} \alpha, & \text{if } \alpha \ge 0^{\circ} \\ \alpha + 360^{\circ}, & \text{if } \alpha < 0^{\circ} \end{cases}.$$

Jointly considering noise reduction, the spatial resolutions and navigation accuracy of VIRR/FY-3A/B, AIRS/Aqua and IASI/Metop-A data, the inter-calibration area is gridded with both Δx and Δy equal to 1.0, and thus the dimensions of the gridded intercalibration area are 61×61. The radiances extracted from VIRR/FY-3A/B L1 products http://fy3.satellite.cma.gov.cn, AIRS/Aqua L1B geo-located and calibrated infrared radiances (Version 5) http://disc.sci.gsfc.nasa.gov/AIRS , and IASI/Metop-A L1C products http://www.class.ngdc.noaa.gov, were pixel-aggregated into the gridded inter-calibration area using an area-weighted interpolation method

$$V_i = \sum_{j=1}^{N} s_{ij} V_j \Big/ \sum_{j=1}^{N} s_{ij} \quad ..(4)$$

where V_i is the output value of the target pixel i, N is the number of input pixels, s_{ij} is the overlapping area between pixels i and j, and V_j is the value of the pixel j.

Based on the tradeoff between uncertainty and the number of matching measurements, the matching criteria are 1) collocation over the gridded intercalibration area, 2) the absolute observation time difference of less than 20 minutes (|Δtime|<20'), and 3) $|\cos\theta_1/\cos\theta_2 - 1| < 0.015$, where θ_1 and θ_2 are the at-surface view zenith angles of VIRR/FY-3 measurement and the hyperspectral measurement, respectively. In order to investigate the impact of solar illumination, the matching measurements were grouped into two categories: with satellites illuminated by the Sun and with satellites in the Earth shadow. Taking the intercalibration of VIRR/FY-3A/B split-window channels against IASI/Metop-A hyperspectral channels as examples, Figures 1 and 2, respectively, shows the qualified matching measurements and linear fits of VIRR/FY-3A/B measurements against the convolved IASI/Metop-A measurements in the channels 4 and 5. VIRR/FY-3A/B measurements are highly linearly related to the matching convolved hyperspectral measurements with the determination coefficients, R^2, greater than 0.99. Against the hyperspectral channels, calibration biases existed in both VIRR/FY-3A/B channels 4 and 5, and presented certain seasonal or annual variations, especially for VIRR/FY-3A channels 4 and 5. No obvious influence of solar illumination on VIRR/FY-3A/B measurements was observed. Generally, when the brightness temperature varies from 220.0 to 300.0 K, the brightness temperature bias in VIRR/FY-3A channel 4 changes from ~5.4 K to ~–0.3 K in June and from ~4.7 K to ~–2.4 K in December, while the brightness temperature bias in VIRR/FY-3A channel 5 goes from ~1.6 K to ~0.0 K, and the brightness temperature bias linearly varies from ~0.8 to ~–0.4 K for VIRR/FY-3B channel 4, whereas it was ~0.3 K for VIRR/FY-3B channel 5. In contrast to VIRR/FY-3A, progress has been made on in-orbit calibration of VIRR/FY-3B split-window channels

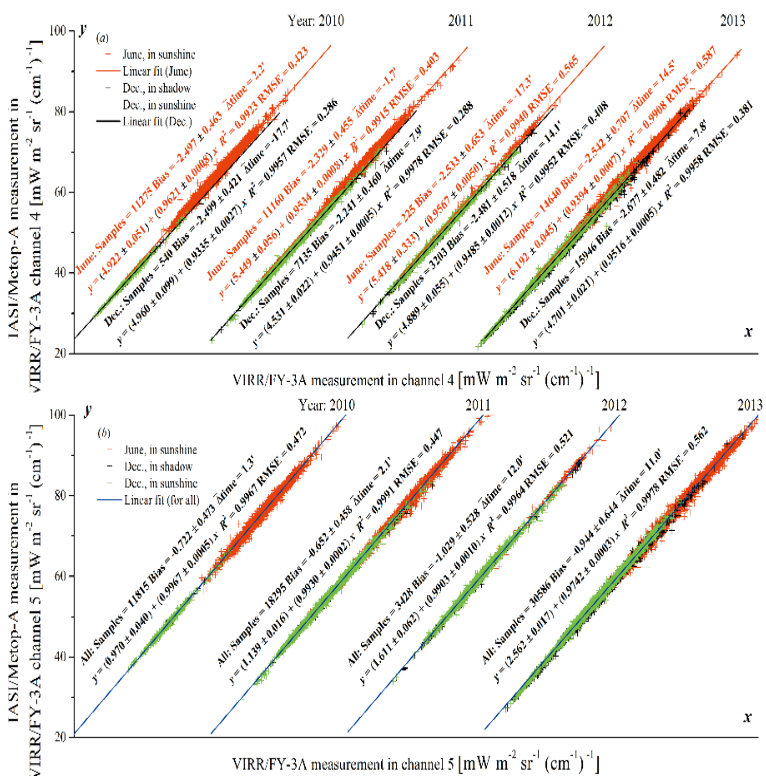

Figure 1. Matching measurements and linear fits of VIRR/FY-3A measurements against the convolved IASI/Metop-A measurements in the channels 4 (*a*) and 5 (*b*) (the red and green crosses are the matching measurements with satellites illuminated by the Sun, whereas the black crosses are the matching measurements with satellites in the Earth shadow. R^2 and RMSE stand for determination coefficient and root mean square error, respectively; Bias is the mean of differences between VIRR/FY-3A and the convolved hyperspectral measurements; $\bar{\Delta}\mathrm{time}$, in minutes, is the mean of observation time differences between the matching VIRR/FY-3A and hyperspectral measurements)

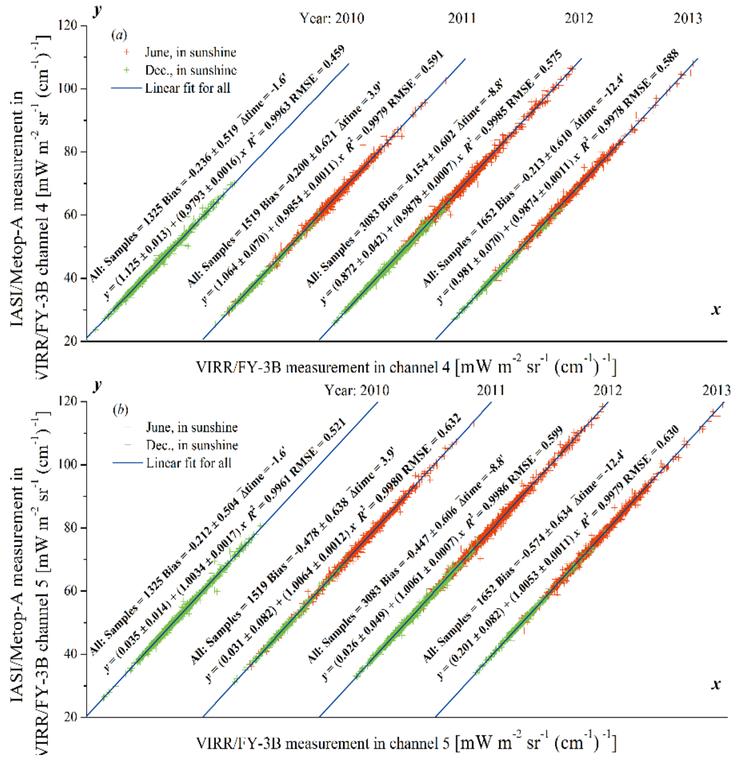

Figure 2. As in Figure 1, but for the matching measurements between VIRR/FY-3B and IASI/Metop-A

References

G.-M. Jiang, 2010: Intercalibration of infrared channels of polar-orbiting IRAS/FY-3A with AIRS/Aqua data. *Optics Express*, vol. 18, no. 4, 3558-3363.

G.-M. Jiang, Z.-Y. Wang and J. Wang, 2016: Intercalibration of VIRR/FY-3A/B split-window channels with AIRS/Aqua and IASI/Metop-A measurements. *International Journal of Remote Sensing*, 37:22, 5249-5269

Discuss the Article

On-orbit Image restoration algorithm to enhance spatial quality of FengYun-3C/MERSI

by Min Min, Guangzhen Cao and Na Xu, Xiuqing Hu (National Satellite Meteorological Center CMA)

FengYun (FY) -3 is a second-generation Chinese meteorological polar-orbit satellite system. FY-3A and -3B were launched as scientific experiment satellites in 2008 and 2011, respectively. As the first operational satellite and FY-3A/B's successor, FY-3C was successfully launched on September 23, 2013, and has maintained stable operations for almost two years. The MEdium Resolution Spectral Imager (MERSI) was installed as a key payload on the FengYun-3C (FY-3C) polar-orbit meteorological satellite. The MERSI sensor onboard FY-3C satellite contains 20 bands with 1.0 and 0.25 km spatial resolutions covering a spectral range varying from visible (VIS, center wavelength at 0.41μm) to long-wave infrared (center wave length at 11.25μm). The key applications of FY-3C/MERSI focus on cloud and aerosol properties, land/sea surface temperature and typhoon monitoring, hence there is a greater emphasis on the on-orbit spatial quality of the imaging system. The spatial quality of the imaging system is quantitatively measured and estimated by the modulation transfer function (MTF) values at the Nyquist frequency. Here, we used fourteen months of continuous FY-3C/MERSI Level-1B data (from November 2013 to December 2014) to evaluate the on-orbit image spatial quality. Based on a polar ice block image, a sharp target modulation transfer function (MTF) estimation method is used to quantitatively estimate the MTF value at the Nyquist frequency (*Min et al., 2014*), which is an index for the spatial quality. The results show very good stability in the first year and a relatively lower spatial quality (MTF approximately 0.15) along the FY-3C/MERSI scan direction (Figure1). This relatively lower spatial quality is primarily attributed to the known and fixed 27% overlapped scan mode of MERSI, which can significantly reduce the image contrast. The original purpose of this design deficiency in FY-3C/MERSI imaging system is to enhance the signal-to-noise ratio (SNR) of image (*Min et al., 2016*).

To enhance spatial quality or contrast of FY-3C/MERSI image along scan direction, we develop a robust image restoration algorithm based on 27% fixed overlapped proportion of MERSI. This fast and robust image restoration algorithm is used to solve the linear equations from the digital number (DN) values of image using the Gaussian elimination (GE) method with lower and upper triangular matrices decomposition (LU) (*Min et al., 2016*). The speed-up ratio of this GE with LU decomposition method can attain a value of 626.30 compared with the traditional GE method when it solves linear equations with 2048 MERSI scan pixels. Currently, an image restoration software for the FY-3/MERSI coded in Fortran under Linux system requires only 6 to 10 S to restore FY-3C/MERSI L1b data with 20 bands.

After the image restoration process, significant enhancement in the image spatial quality along the scan direction for every band of FY-3C/MERSI can be found with an increased MTF value.

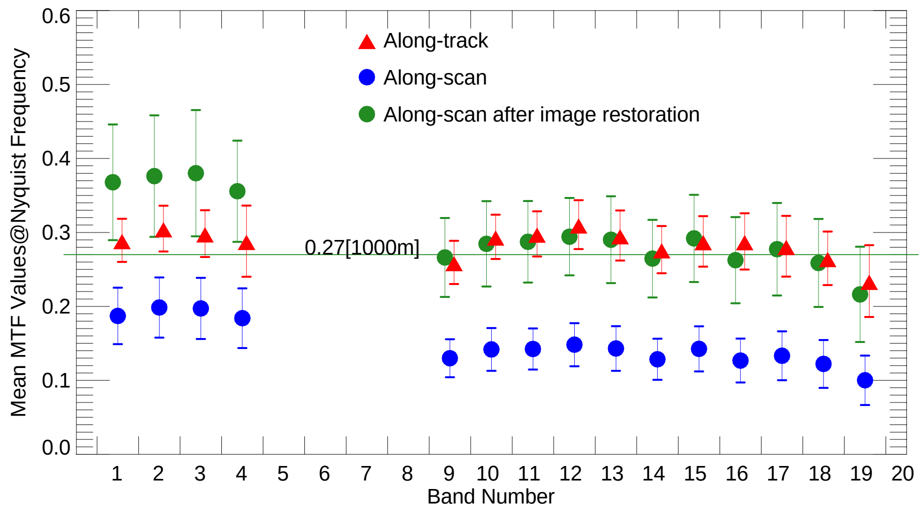

Figure. 1. The averaged MTF values (with standard deviations) at the Nyquist frequency for 15 bands of FY-3C/MERSI sampled along the flight direction (red solid triangle), along the scan direction (blue solid circle), and along the scan direction after the image restoration process (green solid circle)

Figure 1 shows the average (from November 2013 to December 2014) MTF values (with standard deviations) at the Nyquist frequency for the 15 bands of FY-3C/MERSI sampled along the orbital track direction, scan direction, and scan direction after the image restoration process. Evidently, the systematically higher values of MTF, which are approximately equal to 0.30 in every band, can be found in the samples along the track direction. The MTF results of B01-B04 along the scan direction are approximately 0.20, which are higher than those of B09-B19 (by approximately 0.12).

Accordingly, the spatial qualities along the scan direction do not reach the original instrument design target of 0.27 for FY-3/MERSI (*Min et al., 2016*). It is noted that the average MTF value of 0.3 for FY-3C/MERSI is comparable with the long-term averaged MTF of MODIS, which is around 0.35 for Band01-04 (*Choi et al., 2014*). However, we also evaluate the possible effect of this restoration algorithm on the original digital number (DN) and reflectance values. We find a slight decrease in the total averaged DN (0.5) and reflectance (<0.5%, relative bias) values. The variation in DN or reflectance after the image restoration process exhibits a positive correlation with homogeneity of the original target. Moreover, a sensitivity study on the reflectance reveals that it has a more significant impact on the inhomogeneous pixel with a low DN value.

References

Min, M., X. Hu, and Y. Bai (2014), Performance evaluation for on-orbit modulation transfer function of FengYun-3C Medium Resolution Spectral Imager (MERSI) using polar ice and snow, Proc. of SPIE, 9264, 92640M, doi:10.1117/12.2070217.

Min, M., G. Cao, N. Xu, Y. Bai, S. Jiang, X. Hu, L. Dong, J. Guo, and P. Zhang (2016), On-orbit spatial quality evaluation and image restoration of FengYun-3C/MERSI. *TGRS*, 54(12), 6847-6858, doi:10.1109/TGRS.2016.2569038

Choi, T., X. Xiong, and Z. Wang (2014), On-Orbit Lunar Modulation Transfer Function Measurements for the Moderate Resolution Imaging Spectroradiometer, *IEEE TGRS*, 52(1), 270-277

Discuss the Article

Doi: 10.7289/V52805PH

GSICS Quarterly: Winter Issue 2017 Volume 10, No. 4, 2017

News in this Quarter

The seventh Asia/Oceania Meteorological Satellite Users' Conference (AOMSUC-7) held in Songdo, Korea.

by Doheyong Kim, KMA

The seventh Asia/Oceania Meteorological Satellite Users' Conference (AOMSUC-7) was held in Songdo City, Republic of Korea from 24-27 October 2016. The conference was hosted and sponsored by Korea, and was co-sponsored by China, Japan, Australian, the Russian Federation, Indonesia, India, the World Meteorological Organization (WMO), and the Group on Earth Observations (GEO). The conference was held in conjunction with the 2nd AMS-Asia Satellite Conference and the 2nd KMA Meteorological Satellite Users' Conference. Over 230 scientists, users, and satellite operators representing 37 countries participated in the AOMSUC-7. The conference also had a two-day training session. The title of the training was "Capacity Building for Next Generation Meteorological Satellites".

Overall, all three components of the meeting (AOMSUC, AMS and the Training) provided excellent opportunities to share knowledge and learn vital topics on meteorology research and applications some of which are listed in Table 1.

Traditionally the AOMSUC has served as a vital platform for highlighting advances made by the GSICS in satellite monitoring, identify requirements from the Meteorological community and communicate to the community about GSICS products and inter-calibration algorithms and data sets.

AOMSUC-7 Agenda		
Day 1	Opening Address	
	Session 1	Current and Future Meteorological Satellite Programs
	Session 2	Expectations from the Next Generation Satellites and User's Broad Needs in Asia/Oceania.
	Session 3	Preparing the New Generation of Meteorological Satellites
Day 2	Session 4	Program Plans, Data Access and Utilization
	Session 5	Atmospheric Parameters Derived from Satellite Observations
Day 3	Session 6	Application of Satellite Data to Weather Analysis and Disaster Monitoring
	Session 7	Application of Satellite Data to Data Assimilation and Numerical Weather Prediction(NWP)
	Session 8	Application of Satellite Data Calibration / Validation and Climate / Environmental Monitoring
Day 3	Session 9	Land Surface and Ocean Parameters Derived from Satellite Observations
	Session 10	Capacity Building and Training Activities

From a GSICS' standpoint, Session 1, "Current and future meteorological satellite programs," and Session 6, "Application of satellite data to weather analysis and disaster monitoring," were especially interesting. In session 1, Jae-Gwang Won (NMSC, KMA) gave a talk that described KMA GSICS activities to monitor the spectral response of the COMS imager. Won emphasized that more efforts are required for cal/val of geophysical products, including sites and special observatories. KMA is also committed to contribute to systematic generation of ECV records, coordinated in the WMO Sustained Coordinated Processing of Environmental Data Records (SCOPE-CM) initiative. In session 6 Su Jeong Lee (Ewha Woman's University) showed her results using GSICS corrected images for humidity profile retrievals.

Doi: 10.7289/V52805PH

Attendees of the AOMSUC-7

In addition to the GSICS monitoring, the AOMSUC also appreciated the progress in the overarching WMO Integrated Global Observing System (WIGOS) of which GSICS is a component. Under the WIGOS framework, participants welcomed the efforts being undertaken to distribute and utilize the existing and data from future satellites (particularly those by USA, EUMETSAT and China). It is envisaged that future data streams of satellites would be of very high resolution, would be multispectral and in digital format (15 or more channels in the visible to near infrared and across the infrared portion of the spectrum);

- It was agreed that coordination in the generation of new products and services by the Asia/Oceania user community is required to efficiently use the new data streams.
- It also points to the potential need for joint satellite applications facilities as is spelled out in the Memorandum on the AOMSUC signed at WMO EC 2016 (immediately below).
- Following the AOMSUC-7, at the WMO Executive Council on the 16th of June 2016 the AOMSUC was recognized on a formal international basis by the Permanent Representatives to WMO of Australia, China, India, Indonesia, Japan, Korea, the Russian Federation and the Secretary-General of WMO; all confirmed and signed the "*Memorandum on the Asia-Oceania Meteorological Satellite Users Conference (AOMSUC)*". That memorandum established the conference to be held on an annual basis.

In the poster session, over 40 posters detailed new developments in sensor calibration, cloud detection and characterization, wind retrievals, dust detection, fire monitoring, nighttime sea fog detection, convective initiation characterization, rainfall estimation, NWP improvements resulting from satellite data usage, and several other topics. The session produced spirited discussion, initiated new collaborations, and provided further opportunity for useful information exchange.

The Russian Federation announced that they are planning to host the 8th AOMSUC on 16-21 October 2017 and invited prospective attendees to Vladivostok (Detailed Announcement on Page 10.), and Indonesia announced its intentions to host the 9th AOMSUC in a venue to be decided in Indonesia in October of 2018.

Dr. James Purdom, Chair of the ICSC, summarized the Memorandum on the AOMSUC that was signed at WMO EC to continue the AOMSUCs, the mechanisms for continuation, and terms of reference of the hosting institute, co-sponsors, the ICSC and AOMSUC supporting secretariat.

AOMSUC-7 was very successful in meeting the four goals of these conferences; These can be summarized as follows:

1. To promote the importance of satellite observations and highlight their utility
2. To advance satellite remote sensing science by enabling scientist to scientist information exchanges focused on Asia/Oceania,
3. To provide a means for satellite operators to interact directly with the user community concerning current and future satellite related activities and plans, and
4. To engage young people entering the field.

References

http://nmsc.kma.go.kr/aomsuc7/summary.jsp

Discuss the Article

Doi: 10.7289/V52805PH
GSICS Quarterly: Winter Issue 2017 Volume 10, No. 4, 2017

Sentinel-2B: Second 'Color Vision' Satellite for Copernicus launched on 7 March 2017

by Ferran Gascon and Bianca Hörsch (European Space Agency)

The ESA-developed Sentinel-2B satellite has been launched, doubling the coverage of high-resolution optical imaging in the Sentinel-2 mission for the European Union Copernicus environmental monitoring system.
The 1.1 tonne satellite was carried into orbit on a Vega rocket from Europe's Spaceport in Kourou, French Guiana at 01:49 GMT on 7 March (02:49 CET; 22:49 local time, 6 March).
With this launch ESA is taking another step toward advancing the Copernicus programme, which is the most sophisticated Earth observation system in the world. And ESA is planning to add two more satellites to the constellation in the next months: with Sentinel-5P and Sentinel-3B.
The optical imaging Sentinel-2 mission is based on a constellation of two identical satellites: Sentinel-2A, which was launched in June 2015, and Sentinel-2B. Although launched separately, the satellites are placed in the same orbit, flying 180° apart. Every five days, the satellites jointly cover all land surfaces, large islands, and inland and coastal waters between latitudes 84°S and 84°N, optimizing global coverage and data delivery. Each Sentinel-2 satellite carries an innovative high-resolution multispectral camera with 13 spectral bands for a new perspective of land and vegetation. The combination of high-resolution, novel spectral capabilities, a field of vision covering 290 km and frequent revisit times will provide unprecedented views of Earth.

Artist rendition of Sentinel-2B in space, Photo curtsey ESA

Information from this mission is helping to improve agricultural practices, monitor the world's forests, detect pollution in lakes and coastal waters, and contribute to disaster mapping.
Six families of Sentinel satellites will make up the core of EU's Copernicus environmental monitoring network. An EU flagship space initiative, Copernicus provides operational information on the world's land surfaces, oceans and atmosphere to support environmental and security policymaking, and meet the needs of citizens and service providers.

Discuss the Article

Announcements

GSICS Topical Session to be part of AOMSUC-8 at Vladivostok Russia, 16-21st October 2017, Russian Federation

by Alexey Rublev (ROSHYDROMET) and Lawrence E Flynn (NOAA)

The GSICS Users Workshop will return to the AOSMUC in a modified format as a topical session at the 8th Asia/Oceania Meteorological Users Conference (AOMSUC-8). The AOMSUC-8 is organized by ROSHYDROMET and ROSCOSMOS and will be held in Vladivostok, Russia from the 16th to 21st of October 2017. The program session topics include the following:

a) Current and future meteorological satellite programs
b) Facilitation of data access and utilization
c) Atmospheric parameters derived from satellite observations

d) Application of satellite data to weather analysis and disaster monitoring
e) Application of satellite data to numerical weather prediction
f) Application of satellite data for climate and environmental monitoring
g) Land surface and ocean parameters derived from satellite observations
h) Global Spaced-based Inter-Calibration System (GSICS)
i) Capacity building and training activities

The GCC will arrange submission of abstracts for two introductory/overview talks covering GSICS products and applications in Session (h). GSICS products developers and users are invited to submit additional abstracts for the session. The deadline for abstract submission is 31 July 2017. The 1st announcement, online registration form, visa support information and abstract submission information are provided at http://aomsuc8.ntsomz.ru/1-announcement/. Visa applicants should allow at least two months for the process to be completed. The deadline for registration is 30 September 2017 and the 2nd announcement will be available on the website on 30 June 2017. There is no conference fee.

2017 EUMETSAT Satellite conference to be held 2-6th October 2017 in Rome, Italy

by Tim Hewison, EUMETSAT

The 2017 EUMETSAT Meteorological Satellite Conference will take place from 2 to 6 October 2017 in Rome, Italy. The conference will cover the following topics

1) Current and future satellite programmes and instruments
2) New horizons for the Indian Ocean
3) Use of data from current and future satellites in very high-resolution NWP models
4) Atmospheric composition: recent advances in satellite products and applications
5) Marine environment monitoring: recent advances in satellite products and applications
6) Satellite data in support of operational hydrology and water resources management
7) Use of satellite data in climate monitoring
8) Next generation geostationary satellites

REGISTRATION DEADLINES AND FEES:
Registrations submitted by 21 June 2017: early registration fee of €300
Registrations submitted by 5 September 2017: standard registration fee of €350
Registrations submitted after 5 September 2017 and on-site: late registration fee of €450.
The registration website will open in May 2017. Detailed information about the conference can be found at EUMETSAT website at http://www.eumetsat.int/website/home/News/ConferencesandEvents/DAT_3212307.html

GSICS-Related Publications

Currey C, Bartle A, Lukashin C, Roithmayr C, Gallagher J. 2016, Multi-instrument inter-calibration (MIIC) system. *Remote Sens.* **2016**, *8*(11), 902; doi:10.3390/rs8110902

Geng-Ming J, Zhong-Yi, W and Junbang W , 2016.,Intercalibration of VIRR/FY-3A/B split-window channels with AIRS/Aqua and IASI/MetopA measurements, International Journal of Remote Sensing, 37:22, 5249-5269, doi: 10.1080/01431161.2016.1232873

Guo, Q., Chen, F., Chen, B., Feng, X., Yang, C., Wang, X. and Zhang, Z., 2016, Internal-blackbody calibration (IBBC) approach and its operational application in FY-2 meteorological satellites. Q.J.R. Meteorol. Soc., 142: 3082–3096. doi:10.1002/qj.2890 2.

Kozlov, A. A. et al. ,2016., IRFS-2 onboard radiometric calibration errors evaluation by comparison with SEVIRI/Meteosat-10 data. Sovremennye Problemy Distantsionnogo Zondirovaniya Zemli Iz kosmosa, *13*(6), 264–272. doi: 10.21046/2070-7401-2016-13-6-264-272

Menzel, W . et al., 2016, Reprocessing of HIRS satellite measurements from 1980 to 2015: Development toward a consistent decadal cloud record. Journal of Applied Meteorology and Climatology . 2016;55(11):2397–410. doi: 10.1175/JAMC-D-16-0129.1

Smirnov, M .T, 2016., Analysis of measuring capabilities and empirical model of instrumental distortions of ZOND-PP satellite microwave L-band radiometric instrument for calibration and data processing, Sovremennye problemy distantsionnogo zondirovaniya Zemli iz kosmosa, 2016, Vol. 13, No. 6, pp. 273-285,doi: 10.21046/2070-7401-2016-13-6-273-285

Return to Page 1

Submitting Articles to GSICS Quarterly Newsletter:

The GSICS Quarterly Press Crew is looking for short articles (~800 to 900 words with one or two key, simple illustrations), especially related to cal/val capabilities and how they have been used to positively impact weather and climate products. Unsolicited articles are received for consideration anytime, and if accepted, will be published in the next available newsletter issue after approval/editing. Note the upcoming spring issue will be a general issue. Please send articles to manik.bali@noaa.gov.

With Help from our friends:

The GSICS Quarterly Editor would like to thank Xiangqian Wu for the lead article in this issue. Thanks are also due to Tim Hewison, Edward A. Celarier and Sri Harsha Madhavan, for reviewing articles in this issue. Thanks also due to Mrigya Sharma and Anugraha Anand for helping with the image presentation.